Available at: http://www.ictp.it/~pub_off IC/2006/115

United Nations Educational, Scientific and Cultural Organization
and
International Atomic Energy Agency
THE ABDUS SALAM INTERNATIONAL CENTRE FOR THEORETICAL PHYSICS

SOLITON PATTERNS AND BREAKUP THRESHOLDS IN HYDROGEN-BONDED CHAINS

A.S. Tchakoutio Nguetcho[1]
Laboratoire de Mécanique, Département de Physique, Faculté des Sciences, Université de Yaoundé I, B.P. 812, Yaoundé, République du Cameroun

and

T.C. Kofane[2]
Laboratoire de Mécanique, Département de Physique, Faculté des Sciences, Université de Yaoundé I, B.P. 812, Yaoundé, République du Cameroun
and
The Abdus Salam International Centre for Theoretical Physics, Trieste, Italy.

Abstract

We study the dynamics of protons in hydrogen-bonded quasi one-dimensional networks in terms of a diatomic lattice model of protons and heavy ions, with a phi-four on-site substrate potential. We show that the model with linear and nonlinear coupling between lattice sites of the quartic type for the protons admits a richer dynamics that cannot be found with linear coupling. Depending on the two types of physical boundary conditions namely, the drop and condensate types of boundary conditions, and on conditions that require the presence of linear and nonlinear dispersion terms, soliton patterns that are represented by soliton with compact support, peak, drop, bell, cusp, shock, kink, bubble and loop solitons, are derived within a continuum approximation. The phase trajectories, as well as an analytical analysis, provide information on an disintegration of soliton patterns upon reaching some critical values of the lattice parameters. The total energies of soliton patterns are exactly calculated in the displacive limit. We also show that when the phonon anharmonism is taken into account, the width and the energy of soliton patterns are in qualitative agreement with experimental data.

MIRAMARE – TRIESTE

December 2006

[1]nguetchoserge@yahoo.fr
[2]Senior Associate of ICTP. tkofane@uycdc.uninet.cm

1 Introduction

The Transport of protons in hydrogen-bonded systems constitutes a very appealing subject, with the aim of describing nonlinear solitonic excitations which, according to the ideas of Antonchenko, Davydov and Zolotaryuk [1], would be related to the formation and propagation of ionic and Bjerrum defects. These ideas have been in fact successfully tested in a variety of organic as well as inorganic substances that form chains, networks and solids utilizing hydrogen-bonding mechanisms, as, for example, Ice and hydrogen halides which are the best known examples of inorganic hydrogen-bonded solids [2, 3, 4], whereas proteins, DNA, and other biological macromolecules are examples of organic hydrogen-bonded chains [5, 6]. The protonic conductivity is usually associated with the motion along a hydrogen-bonded chain of ionic(ionization) and Bjerrum (orientational or bonding) defects [4, 7]. The former involve translational motions of the hydrogen-bonded protons, whereas the latter are results of rotations of the hydroxyl ions or some other hydroxyl groups. The transport of protons may begin either with the passage of an ionic defect or the passage of an orientational defect, but thereafter the motion of these defects must strictly alternate [5, 6, 8, 9]. In addition, it has been demonstrated that many biological activities, such as photosynthesis, repair mechanism of DNA after radiation damage, metabolism, signal transduction in cells, enzymatic processes, and respiration which are driven by electron transfer reactions [10, 11], may proceed along a single pathway which, as the preferred channel for electron transfer reactions, can be established by a hydrogen-bonded strand within the secondary structure [12, 13]. One of the questions that has been raised for the mechanism of proton conductivity is regarding the roles played by the nonlinear on-site potential for the protons, leading to the three scenarios: (1) the model usually consists of two interacting sublattices:one of harmonically coupled light ions(protons) with a doubly degenerate nonlinear on-site potential of phi-four type and the other of harmonically coupled heavy ions. The theories differ in choosing the form of the interaction between the two sublattices. Usually, a nonlinear coupling between the two sublattices are considered [14, 15], although there are models which consider a linear coupling [16, 17]. (2) The doubly degenerate nonlinear on-site potential is of the double-Morse type. In fact, as shown by quantum chemistry calculation [18, 19, 20], a good approximation of the double-well potential can be constructed as the superposition of two symmetrically situated ion-proton Morse potential as well as an ion-ion coupling [21, 22, 23, 24, 25, 26, 27, 28, 29]. (3) The nonlinear on-site potential is of the double sine-Gordon type with nonlinear [30, 31] and linear [32] couplings. In the first two cases, models are able to describe energy transport, dielectric polarization, and proton storage in hydrogen-bonded networks but they are unable to explain the protonic mass in such a system that is necessary to support the saturated protonic conductivity in ice and other hydrogen-bonded semiconductors [33]. In the last case, models can explain simultaneously the ionic and Bjerrum defects formation and propagation using well-known soliton properties [30, 31, 32]. Besides the nonlinear on-site potential for the protons, hydrogen-bonded

models with phonon anharmonisms occur too. First, such a model was introduced by adding higher-order terms such as the cubic and quartic anharmonicities to the harmonic potential [34, 35, 36, 37, 38, 39]. Later, it was introduced with an exponential nonlinearity, represented by, e.g., Morse, Toda or Lennard-Jonnes potentials [40, 41, 42, 43, 44].

The solitons which appeared in those models are well known as solutions supported by the balance of dispersion and nonlinear effects. The presence of the solitons with infinite tails is at the origin of mutual interactions between adjacent solitons, even at great distances. For example, in nonlinear optical fiber optics, this long-range interaction imposes a strict limitation on the performance of long-haul fiber transmissions [45]. Recently, It has been shown that the inclusion of anharmonicities in the study of lattice models can produce qualitatively new effects. In particular, Rosenau and Hyman [46] found solutions of the solitary type without infinite tails, termed solitons with compact support or compactons [46, 47, 48, 49, 50, 51]. In other words, two adjacent compactons do not interact unless they come into contact in a way similar to the contact between hard spheres. It has been shown that the effects of lattice discreteness, and the presence of a linear coupling between lattice sites are detrimental to a stable ballistic propagation of the compacton, because of the particular structure of the small oscillation frequency spectrum of the compacton in which the lower frequency internal modes enter in direct resonance with phonon modes [47]. The existence of a localized breathing mode with a compact support has been demonstrated [48]. A quantization condition of the values of the width parameter of the discrete compacton has been proposed [50].

The aim of this paper is to investigate the properties of the one-dimensional diatomic chain of protons and heavy ions, where the proton dynamics is influenced by anharmonic lattice vibrations. Except the work by Kashimori, Kikushi and Nishimoto [37], our anharmonic treatment of the lattice vibrations goes beyond the usual harmonic approximation of a two-sublattice soliton model of the hydrogen-bonded proton Hamiltonians [1, 30, 33]. In this model with quartic nonlinear proton-proton coupling, we consider conditions that require the presence of nonlinear dispersion as well as linear dispersion. We show in this paper that soliton pattern mechanisms that require a nonlinear coupling of the protons in adjacent hydrogen bonds may exist if one properly choose the types of physical boundary conditions. The soliton patterns that we obtain are solitons with compact support, without infinite tails rather than the kinks with infinite tails in the coupled double-well model.

The paper is organized as follows. In section 2, we present the model Hamiltonian of one-dimensional interacting two-sublattice model of anharmonically coupled protons and harmonically coupled heavy ions. By using two types of physical boundary conditions namely, the drop and condensate types of boundary conditions, we obtain in the continuum limit two-component compactonlike solutions and calculate the total energy concentrated in each solutions. Analytic expressions for the dependence of the breakdown threshold value on the nonlinear parameter, on the constant coupling between the two sublattices, and on the velocity of the soliton patterns

are derived. The last section contains a summary and conclusions.

2 Description of the Model and Analytical Results

2.1 Description of the Model

A typical one-dimensional hydrogen-bonded network consists of two coupled sublattices $\cdots X-H\cdots X-H\cdots X-H\cdots X-H\cdots$, where the hydrogen atom H (or proton H^{+}) with the mass m, in each lattice unit, is connected with its adjacent heavy ions or more generally hydroxyl groups X or (X^{-}) via either a covalent $(-)$ or a hydrogen $(\cdots)$ bond which the mass is M $(m<M)$, forming a hydrogen bonded bridge $X-H\cdots X$ [1, 37]. The covalent and hydrogen bonds in a $X-H\cdots X$ configuration are interchangeable, viz., the proton in the bond that links the two X ions together can tunnel between two equilibrium positions that are energetically equivalent. Thus, the nature of the effective potential for proton is that with two stable equilibrium positions separated by unstable one. A typical example of such a potential for the proton in the hydrogen bond is the well-known double-well potential [1] expressed by:

$$V\left(u_n\right)=V_0V_{\mathrm{sub}}\left(u_n\right)\ , \tag{1}$$

with

$$V_{\mathrm{sub}}\left(u_n\right)=\left(1-\frac{u_n^2}{u_0^2}\right)^2\ , \tag{2}$$

where u_n denotes the displacement of the nth proton with respect to the center of the heavy-ion pair, V_0 the potential barrier, and $2u_0$ is the distance between the two minima of the double-well potential, as illustrated in Fig.(1). Thus, the Hamiltonian of the proton sublattice is [37]:

$$H_1=\sum_n\left[\frac{1}{2}m\left(\frac{du_n}{dt}\right)^2+V\left(u_n\right)+\frac{1}{2}mC_0^2\left(u_{n+1}-u_n\right)^2+\frac{1}{4}mC_a\left(u_{n+1}-u_n\right)^4\right]\ , \tag{3}$$

where the two last terms represent the harmonic and anharmonic couplings, respectively, with C_0, the characteristic velocity and C_a, the anharmonic coupling parameter between neighboring protons. The Hamiltonian of the heavy-ion sublattice is [53]

$$H_2=\sum_n\frac{1}{2}M\left(\frac{dy_n}{dt}\right)^2+\frac{1}{2}Mv_0^2\left(y_{n+1}-y_n\right)^2\ , \tag{4}$$

where the last term describes an harmonic coupling between neighboring heavy ions pairs. The last part of the Hamiltonian of the model H arises from the dynamical interaction between two sublattices and describes the modulation of the double-well potential caused by the variation of the distance between the heavy ion that surrounds a small one and which is given by [53]:

$$H_3=\sum_n\chi\left(y_{n+1}-y_n\right)\left(u_0^2-u_n^2\right)\ , \tag{5}$$

where χ measures the strength of the coupling between the two interacting sublattices. From the total Hamiltonian ($H = H_1 + H_2 + H_3$), one can derive, in dimensionless form, the equations of motion as follows:

$$m\left(\frac{d^2u_n}{dt^2}\right) = mC_0^2\left(u_{n+1}+u_{n-1}-2u_n\right)+mC_a\left[\left(u_{n+1}-u_n\right)^3+\left(u_{n-1}-u_n\right)^3\right]+ \quad (6)$$
$$+2\chi u_n\left(y_{n+1}-y_n\right)-V_0\frac{dV_{\rm sub}(u_n)}{du_n}$$

$$M\left(\frac{d^2y_n}{dt^2}\right) = mv_0^2\left(y_{n+1}+y_{n-1}-2y_n\right)+\chi\left(u_{n-1}-u_n\right)\left(u_{n-1}+u_n\right) \quad (7)$$

These sets of Eqs. (6) and (7) are not solvable analytically. The classical approach to this problem is to assume that the coupling between neighboring sites is sufficiently strong. Thus, the discrete variables $u_n(t)$, and $y_n(t)$ can be replaced by two continuous functions of space and time $u(x=na,t)$, $y(x=na,t)$, and under this continuum approximation, Eqs. (6) and (7) become,

$$m\left(\frac{d^2u}{dt^2}\right) = ma^2C_0^2\left(\frac{d^2u}{dx^2}\right)+3ma^4C_a\frac{d^2u}{dx^2}\left(\frac{du}{dx}\right)^2+2a\chi u\left(\frac{dy}{dx}\right)-V_0\frac{dV_{\rm sub}(u)}{du} \quad (8)$$

$$M\left(\frac{d^2y}{dt^2}\right) = Ma^2v_0^2\left(\frac{d^2y}{dx^2}\right)-2a\chi u\left(\frac{du}{dx}\right) \quad (9)$$

where a is the lattice parameter.

2.2 Soliton Excitations

We now turn our attention to the traveling wave solutions. For the sake of convenience, we can look solution with constant profile moving at the velocity v. Thus, Eq. (8) and Eq. (9) in the moving frame as a function of the moving dimensionless $s = \dfrac{x-vt}{a}$ yield,

$$\left[1-V_1^2+3C_{nl}\left(\frac{du}{ds}\right)^2\right]\left(\frac{d^2u}{ds^2}\right) = \lambda\frac{dV_{\rm sub}(u)}{du}-2\chi_1 u\left(\frac{dy}{ds}\right) \quad (10)$$

$$\left(1-V_2^2\right)\left(\frac{d^2y}{ds^2}\right) = 2\chi_2 u\left(\frac{du}{ds}\right) \quad (11)$$

where $V_1 = \dfrac{v}{aC_0}$ and $V_2 = \dfrac{v}{av_0}$ are the scaled (dimensionless) soliton velocities of protons and heavy-ions, respectively. $C_{\rm nl}$ is the parameter that control the strength of the nonlinear coupling and is related to the anharmonical coupling coefficient C_a by the relation $C_{\rm nl} = \dfrac{C_a}{C_0^2}$, while $\chi_1 = \dfrac{\chi}{mC_0^2}$, and $\chi_2 = \dfrac{\chi}{Mv_0^2}$, are the parameters that control the strength of the coupling between the two interacting sublattice, and $\lambda = \dfrac{V_0}{mC_0^2}$, denotes the scaled amplitude of the periodic potential and measures the effective depth of the potential of the proton. Integrating Eq. (11), we obtain

$$\frac{dy}{ds} = \frac{\chi_2}{\left(1-V_2^2\right)}u^2+K_1 \quad (12)$$

where K_1 is a constant of integration which can be determined by the boundary conditions. To determine this constant, we have used two types of boundary conditions namely, the trivial (drop) type of boundary conditions and the classical (condensate) type boundary conditions.

2.2.1 Soliton excitations with drop type of boundary conditions

This type of boundary conditions are appropriate for drop and peak soliton solutions [28], and are determined by the expressions

$$\begin{aligned} \frac{du}{ds} &\longrightarrow 0, \quad u \longrightarrow 0, \quad as \quad s \longrightarrow \pm\infty \\ \frac{dy}{ds} &\longrightarrow 0, \quad as \quad s \longrightarrow \pm\infty \end{aligned} \tag{13}$$

Introducing Eq. (12) with the boundary conditions given by Eq. (13), into Eq. (10), one obtains

$$\left[1 - V_1^2 + 3C_{nl}\left(\frac{du}{ds}\right)^2\right]\left(\frac{d^2u}{ds^2}\right) = \lambda\frac{dV_{\text{sub}}(u)}{du} - \frac{2\chi_1\chi_2}{\left(1-V_2^2\right)}u^3 \tag{14}$$

The solutions of Eq.(14) can be best analyzed in the phase plane $\left(u, \frac{du}{ds}\right)$. Thus, this equation (14) can be treated as an autonomous dynamic system given by

$$\frac{dp}{du} = \frac{1}{p\left(1 - V_1^2 + 3C_{nl}p^2\right)}\left[\lambda\frac{dV_{\text{sub}}(u)}{du} - \frac{2\chi_1\chi_2}{\left(1-V_2^2\right)}u^3\right] \tag{15}$$

where the derivative $p = \dfrac{du}{ds}$, describes the elongation of the energy bonds in the system. The first integral of this equation, describing the phase portraits of the dynamic system [see Eq. (6)], may be easily obtained with the boundary given by conditions Eq. (13) and which can be written as [52]

$$p^4 - 2p_0^2p^2 = \alpha\left(u^4 - 2\beta u^2\right) \tag{16}$$

where $p_0 = \sqrt{\dfrac{V_1^2-1}{3C_{\text{nl}}}}$, $\alpha = \dfrac{4\lambda\left(V_2^2+\eta-1\right)}{3C_{\text{nl}}u_0^4\left(V_2^2-1\right)}$, $\beta = \dfrac{u_0^2\left(V_2^2-1\right)}{V_2^2+\eta-1}$ with $\eta = \dfrac{\chi_1\chi_2u_0^4}{2\lambda}$. It is clear from the nonlinear equation (16) that, the system carries out symmetrical oscillations of low amplitude around the single stable equilibrium point $(0,0)$, when $\eta > 1$ with $V_2 \in\,]0;1[$, or when $\eta < 1$ with $V_2 \in\,]V_{22};1[$, where $V_{22} = \sqrt{1-\eta}$, and for positive values of C_{nl} [as illustrated in Fig.(2)]. In such case, there is no double-well potential. There is only one minimum of the potential and thus no localized soliton solution exists in this case.

But when $C_{\text{nl}} < 0$, this stable position is transformed into unstable one, and any movement of the system can involve the destruction of the structure.

For $\eta > 1$ and $V_2 \in\,]1;\infty[$, or for $\eta < 1$ and $V_2 \in\,]0;V_{22}[\,\cup\,]1;\infty[$, the system admits three equilibrium positions including two unstable $\left[\left(-\sqrt{\beta},0\right)\right.$ and $\left.\left(\sqrt{\beta},0\right)\right]$, and one stable $(0,0)$ positions. Thus, the system carries out oscillations of low amplitude around the single stable equilibrium point $(0,0)$. Beyond the top of certain values of the amplitude, unlimited

movements occur, leading to the destruction of the system [see Fig.(3 *a*)]. However, when $C_{\rm nl}$ takes the negative value, the system can, under the same conditions, carry out two types of oscillations: oscillations of small amplitudes around the stable points $\left(-\sqrt{\beta},0\right)$ and $\left(\sqrt{\beta},0\right)$, or oscillations of very large amplitudes going until wrapping the two stable positions [see Fig.(3 *b*)]. When $C_{\rm nl}$ increases upon reaching the threshold value

$$C_{\rm nl_{cr1}} = \frac{\left(V_2^2+\eta-1\right)\left(V_1^2-1\right)^2}{12\lambda\left(V_2^2-1\right)}\ , \tag{17}$$

the phase portraits change qualitatively. Indeed, the singular points are almost present in the phase plane plots. One can note the disappearance of the separatrix, indicating the disintegration of soliton solutions as illustrated by Fig.(4 *a*) and Fig.(4 *b*). As one can readily see from Eq. (17), the threshold values depend on the soliton velocities of protons and heavy-ions, the nonlinear parameter and on the effective depth of the potentials of the protons. Now, to solve Eq.(16), we introduce the following condition

$$\left(V_2^2+\eta-1\right)\left(1-V_1^2\right)^2 - 12\lambda C_{\rm nl}\left(V_2^2-1\right) = 0 \tag{18}$$

for which soliton patterns are available. After some lengthy algebra, analytical solutions have been obtained which for the sake of clarity, are present in the following manner.

2.2.1.1 *Peak solitons (peakons)*

These solutions appear when Eq. (16) is solved using Eq. (18). For the motion of the proton, the solution describing a single peak soliton defined by merging the two solution branches is:

$$u = \exp\left[\pm\frac{p_0}{\sqrt{\beta}}\left(s-s_0\right)\right] \tag{19}$$

The solution for the heavy-ions motion can be easily obtained by inserting Eq. (19) into Eq. (12) using the boundary conditions (13), leading to

$$y = \pm\frac{\chi_2\sqrt{\beta}}{4p_0(1-V_2^2)}\exp\left[\pm\frac{2p_0}{\sqrt{\beta}}\left(s-s_0\right)\right] \tag{20}$$

The graphics that represent these solutions are depicted in Fig.(5 *a*).

2.2.1.2 *Drop compactons*

These names are introduced to designate solutions that usually have the form of hump solitons but are defined now only in a finite space sector, and because of their forms and properties which are reminiscent of hard spheres [52]. The proton waveform is given by

$$u = \pm\sqrt{2\beta}\sin\left[\frac{p_0}{\sqrt{\beta}}\left(s-s_0\right)\right] \tag{21}$$

and the heavy-ion waveform is given by

$$y = \frac{\beta\chi_2}{2(V_2^2-1)}\left[\left(s-s_0\right)-\frac{\sqrt{\beta}}{2p_0}\sin\left[\frac{2p_0}{\sqrt{\beta}}\left(s-s_0\right)\right]\right] \tag{22}$$

In Fig.(5 b), we present the double solution for the two sublattices. The width of this drop soliton can be evaluated and has the form

$$L_{drop} = \pi \frac{\sqrt{\beta}}{p_0}.$$

By taking into account Eq.(18), it was obvious to notice that this width of the drop soliton is independent of the parameter of anharmonicity $C_{\rm nl}$ and the parameter of coupling of the two sublattices χ. On the other hand, the latter believes with the speed of the particles of the proton V_1 and decreases with the effective depth of the potential of substrate λ. We also notice that, the amplitude of this type of wave varies with the propagation velocity V_2 of the heavy-ions and the parameter of coupling χ (for a fixed value of V_2, the amplitude decreases when the force of coupling of the two sublattices increases). In the following, we evaluate the energy of these configurations. The total energy of our soliton patterns can be calculated by inserting the explicit solutions into the expression for the Hamiltonian density, that is:

$$E_{\rm total} = mC_0^2 E_1 + Mv_0^2 E_2 + \chi E_3 \tag{23}$$

with

$$\begin{aligned} E_1 &= \int_{-\infty}^{+\infty} \left[\frac{1}{2}\left(1+V_1^2\right)\left(\frac{du}{ds}\right)^2 + \frac{1}{4}C_{\rm nl}\left(\frac{du}{ds}\right)^4 + \lambda V_{\rm sub}\left(u\right)\right] ds, \\ E_2 &= \int_{-\infty}^{+\infty} \frac{1}{2}\left(1+V_2^2\right)\left(\frac{dy}{ds}\right)^2 ds, \\ E_3 &= \int_{-\infty}^{+\infty} \left(u_0^2-u^2\right)\left(\frac{dy}{ds}\right) ds. \end{aligned} \tag{24}$$

By using the above expression, while taking into account of Eq. (18), we obtain:

$$\begin{aligned} E_1 &= \frac{p_0 u_0^2\left(1+V_1^2\right)}{2\sqrt{\beta}} + \frac{C_{\rm nl}p_0^3 u_0^4}{8\beta^{\left(\frac{3}{2}\right)}} - \frac{\lambda u_0^2\sqrt{\beta}\left(u_0^2-4\beta\right)}{2p_0} \\ E_2 &= \frac{u_0^4\chi_2^2\sqrt{\beta}\left(1+V_2^2\right)}{4p_0\left(1-V_2^2\right)^2} \\ E_3 &= \frac{\chi_2 u_0^4\sqrt{\beta}}{2p_0\left(1-V_2^2\right)} \end{aligned} \tag{25}$$

for the peak soliton and,

$$\begin{aligned} E_1 = {} & \frac{p_0\left(1+V_1^2\right)}{\sqrt{\beta}}\left[u_0\sqrt{\beta-u_0^2} + \beta\arcsin\left(\frac{u_0}{\sqrt{\beta}}\right)\right] + \frac{C_{\rm nl}p_0^3}{2\beta^{\left(\frac{3}{2}\right)}}\left[2u_0\left(\beta-u_0^2\right)^{\left(\frac{3}{2}\right)} + 3u_0\beta\sqrt{\beta-u_0^2}\right] + \\ & + 3\beta^2\arcsin\left(\frac{u_0}{\sqrt{\beta}}\right) \\ E_2 = {} & \frac{\chi_2^2\left(1+V_2^2\right)\sqrt{\beta}}{p_0\left(V_2^2-1\right)^2}\left[3\beta^2\arcsin\left(\frac{u_0}{\sqrt{\beta}}\right) - 2u_0^3\sqrt{\beta-u_0^2} - 3u_0\beta\sqrt{\beta-u_0^2}\right] \\ E_3 = {} & \frac{2\chi_2\beta^{\left(\frac{3}{2}\right)}}{p_0\left(V_1^2-1\right)}\left[3u_0\beta\sqrt{\beta-u_0^2} + \left(2u_0^2-3\beta\right)\arcsin\left(\frac{u_0}{\sqrt{\beta}}\right)\right] \end{aligned} \tag{26}$$

for the drop soliton, respectively.

2.2.2 Soliton excitations with condensate type of boundary conditions

The condensate type of boundary conditions are defined by the relation

$$\begin{aligned} \frac{du}{ds} &\longrightarrow 0, \quad u \longrightarrow u_{\min}, \quad as \quad s \longrightarrow \pm\infty \\ \frac{dy}{ds} &\longrightarrow 0, \quad as \quad s \longrightarrow \pm\infty. \end{aligned} \tag{27}$$

where $u_{\min}$ is the minimum of the substrate potential $V(u)$. These types of boundary conditions are appropriated for kink, cusp, peak, and shock soliton solutions. Introducing Eq. (12) with condition (27), into Eq. (10), one obtains,

$$\frac{d^2u}{ds^2} = \frac{1}{\left[1 - V_1^2 + 3C_{\rm nl}\left(\frac{du}{ds}\right)^2\right]}\left[\lambda\frac{\partial V_{\rm sub}(u)}{\partial u} - \frac{2\chi_1\chi_2}{\left(1-V_2^2\right)}u\left(u^2 - u_{\min}^2\right)\right] \tag{28}$$

and the first integral of Eq. (28), describing the phase portraits of the dynamic system, may be easily obtained and is given by the relation

$$p^4 - 2p_0^2p^2 = \alpha\left(u_0^2 - u^2\right)^2. \tag{29}$$

From equation (29), under $V_2 \neq V_{22}$, the classical equilibrium points (corresponding to the extrema of the potential and characteristic for the harmonic interparticle potential system) will always exist. When $\eta > 1$ with $V_2 \in \,]0;1[$, or when $\eta < 1$ with $V_2 \in \,]V_{22};1[$, the dynamic behavior of the system is described by a limited bistable potential. On the other hand, when $\eta > 1$ with $V_2 \in \,]1;\infty[$, or when $\eta < 1$ with $V_2 \in \,]0;V_{22}[\cup]1;\infty[$, the system can make small oscillations around $(0,0)$, and around certain values of the amplitudes, one notices its rupture. All these results have been obtained for positive values of $C_{\rm nl}$. When the latter takes negative values, the bistable system becomes catastrophic and vice versa. Similarly, in the case of the trivial (drop) type of boundary conditions (13), the separatrix, representing the soliton solutions, and relating $u_{\min 1}$ to $u_{\min 2}$, exists for values of $C_{\rm nl}$ lower than the threshold

$$C_{\rm nl_{cr2}} = \frac{\left(1-V_2^2\right)\left(1-V_1^2\right)^2}{12\lambda\left(V_2^2+\eta-1\right)}, \tag{30}$$

and goes away for values of $C_{\rm nl}$ higher than the latter as in Fig.(6 a) and Fig.(6 b), respectively, where $u_{\min 1}$ is one minimum of the substrate potential and $u_{\min 2}$ another one adjacent to $u_{\min 1}$.

Besides these points , few more singular points appear for the drop and condensate types of boundary conditions when $V_1 \in \,]1;\infty[$ and $C_{\rm nl} > 0$, or when $V_1 \in [0;1]$ and $C_{\rm nl} < 0$. The exact position of these new points may be derived from the singularity arising in the denominator of Eq. (15) and Eq. (28). These new points have exactly, at the same conditions as previously, the same X-coordinates as those obtained previously. The main difference is the addition of two new ordinates $-p_0$ and p_0 (characteristic impulse of the system) beside the one given by $p = 0$ [see Figs.(4) and Figs.(6)]. When the model parameters satisfy the relation:

$$\left(V_2^2-1\right)\left(1-V_1^2\right)^2 + 12\lambda C_{\rm nl}\left(V_2^2+\eta-1\right) = 0 \tag{31}$$

the implicit solutions describing the displacement of the protons can be written as:

$$\pm\frac{\sqrt{2}p_0}{u_0}\left(s_{ltn}-s_0\right)=\arcsin(\frac{l}{\sqrt{2}}\frac{u}{u_0})+ln\left[t\sqrt{1-\frac{1}{2}\left(\frac{u}{u_0}\right)^2}+\frac{n}{\sqrt{2}}\frac{u}{u_0}\right] \tag{32}$$

where ln is the neperian logarithm, $l=\pm1$, $t=\pm1$, $n=\pm1$ and these symbols simply indicate the sign of each denoted term on the right-hand side of Eqs. (32) and s_0 is defined by the chosen initial condition. According to Eq. (27), we have four pairs of defined boundary conditions and each pair produces two branches to construct the solutions. Since each branch of the solution travels with the same velocity, the necessary gap Δ in the space s for coalescing solutions, determined by the initial conditions, can be presented in the two types [$\Delta_1=0$ and $\Delta_2=\arcsin(1)$]. Let us first take some solutions when they merge in the "space" with Δ_2. For the boundary condition

$$u\to-u_0 \text{ while } s\to-\infty, \text{ and } u\to u_0 \text{ while } s\to\infty. \tag{33}$$

The solitonic structure can be defined by

$$\frac{\sqrt{2}p_0}{u_0}\left(s_{+--}+\frac{\pi}{2}\right) \text{ if } \frac{\sqrt{2}p_0}{u_0}s\in\left]-\infty,0\right], \text{ and } -\frac{\sqrt{2}p_0}{u_0}\left(s_{---+}-\frac{\pi}{2}\right) \text{ if } \frac{\sqrt{2}p_0}{u_0}s\in[0,\infty[\ .$$

This relation, represented as picture in Fig.(7) is usually referred to as shock wave, has an energy of existence given by the Eq. (23) with

$$\begin{aligned}
E_1 &= \sqrt{2}\left(\frac{1}{2}-\frac{\pi}{8}\right)\left(1+V_1^2\right)u_0p_0+\frac{\sqrt{2}C_{\rm nl}u_0p_0^3}{8}\left(\frac{5}{2}-\frac{3\pi}{4}\right)+\frac{\sqrt{2}u_0\lambda}{p_0}\left(\frac{3}{4}-\frac{\pi}{8}\right), \quad (34)\\
E_2 &= \frac{\sqrt{2}u_0^5\chi_2^2\left(1+V_2^2\right)(6-\pi)}{16p_0\left(V_2^2-1\right)^2},\\
E_3 &= \frac{\sqrt{2}\chi_2u_0^5(6-\pi)}{8p_0\left(V_2^2-1\right)}.
\end{aligned}$$

For the boundary condition

$$u\to-u_0 \text{ while } s\to-\infty, \text{ and } u\to-u_0 \text{ while } s\to\infty, \tag{35}$$

the solitonic structure can be defined by

$$\frac{\sqrt{2}p_0}{u_0}\left(s_{-++}+\frac{\pi}{2}\right) \text{ if } \frac{\sqrt{2}p_0}{u_0}s\in\left]-\infty,\frac{\pi}{2}\right], \text{ and } -\frac{\sqrt{2}p_0}{u_0}\left(s_{-++}+\frac{\pi}{2}\right) \text{ if } \frac{\sqrt{2}p_0}{u_0}s\in\left[-\frac{\pi}{2},\infty\right[\ .$$

$$\frac{\sqrt{2}p_0}{u_0}\left(s_{+++}-\frac{\pi}{2}\right) \text{ if } \frac{\sqrt{2}p_0}{u_0}s\in\left]-\infty,0\right], \text{ and } -\frac{\sqrt{2}p_0}{u_0}\left(s_{+++}-\frac{\pi}{2}\right) \text{if } \frac{\sqrt{2}p_0}{u_0}s\in[0,\infty[$$

The first pair is a loop soliton [see Fig.(8 *a*)] whose energy is divergent and the second is another wave which represents peak soliton [see Fig.(8 *b*)], whose energy is given by Eq. (23), with

$$\begin{aligned}
E_1 &= \sqrt{2}\left(\frac{3\pi}{8}+\frac{1}{2}\right)\left(1+V_1^2\right)u_0p_0+\frac{\sqrt{2}C_{\rm nl}u_0p_0^3}{8}\left(\frac{5}{2}+\frac{9\pi}{4}\right)+\frac{3\sqrt{2}u_0\lambda}{p_0}\left(\frac{1}{4}+\frac{\pi}{8}\right), \quad (36)\\
E_2 &= \frac{3\sqrt{2}u_0^5\chi_2^2\left(1+V_2^2\right)(2+\pi)}{16p_0\left(V_2^2-1\right)^2},\\
E_3 &= \frac{3\sqrt{2}\chi_2u_0^5(2+\pi)}{8p_0\left(V_2^2-1\right)}.
\end{aligned}$$

Let us now consider the case where solutions are specially obtained by coalescing two branches of each pair solution in Eqs. (32), for the second type of nonzero gap Δ_1. For the boundary condition

$$u \to u_0 \text{ while } s \to -\infty, \text{ and } u \to u_0 \text{ while } s \to \infty, \tag{37}$$

the solitonic structure can be defined by

$$\frac{\sqrt{2}p_0}{u_0}s_{-+-} \text{ if } \frac{\sqrt{2}p_0}{u_0}s \in]-\infty, 0] \text{, and } -\frac{\sqrt{2}p_0}{u_0}s_{-+-} \text{ if } \frac{\sqrt{2}p_0}{u_0}s \in [0, \infty[\text{ ,}$$

$$\frac{\sqrt{2}p_0}{u_0}s_{++-} \text{ if } \frac{\sqrt{2}p_0}{u_0}s \in]-\infty, 0] \text{, and } -\frac{\sqrt{2}p_0}{u_0}s_{++-} \text{ if } \frac{\sqrt{2}p_0}{u_0}s \in [0, \infty[\text{ .}$$

The corresponding pattern structures are plotted in Fig.(9), and exist as excitations in condensate state, like a rarefaction of the field. Their forms suggest the names peak bubble and cusp bubble, respectively.

The energy of the peak bubble is given by Eq. (23), with

$$\begin{aligned} E_1 &= \frac{\pi\sqrt{2}\left(1+V_1^2\right)u_0p_0}{8} + \frac{3\sqrt{2}C_{\rm nl}u_0p_0^3}{16}\left(\frac{\pi}{2}-1\right) + \frac{\sqrt{2}u_0\lambda}{8p_0}\left(6+\pi\right), \\ E_2 &= \frac{\sqrt{2}u_0^5\chi_2^2\left(1+V_2^2\right)\left(6+\pi\right)}{16p_0\left(V_2^2-1\right)^2}, \\ E_3 &= \frac{\sqrt{2}\chi_2u_0^5\left(6+\pi\right)}{8p_0\left(V_2^2-1\right)}. \end{aligned} \tag{38}$$

whereas the energy of the cusp diverges.

For the boundary condition given by Eq. (33), the solutions are

$$\frac{\sqrt{2}p_0}{u_0}s_{+++} \text{ if } \frac{\sqrt{2}p_0}{u_0}s \in]-\infty, 0] \text{, and } -\frac{\sqrt{2}p_0}{u_0}s_{-+-} \text{ if } \frac{\sqrt{2}p_0}{u_0}s \in [0, \infty[$$

$$\frac{\sqrt{2}p_0}{u_0}s_{+++} \text{ if } \frac{\sqrt{2}p_0}{u_0}s \in \left]-\infty, \frac{\pi}{2}\right] \text{, and } -\frac{\sqrt{2}p_0}{u_0}s_{--+} \text{ if } \frac{\sqrt{2}p_0}{u_0}s \in \left[\frac{\pi}{2}, \infty\right[\text{ ,}$$

and are represented in Fig.(10).

These are topological kinklike solitons, solutions very often used to interpret and to explain the process of the transfer of protons in hydrogen-bonded systems. The second one has a little peak near the center and can be interpreted as domain a traveling along the medium. The energy of kinklike solitons, which consists of kinetic and potential terms, can be calculated from Eqs. (23), with

$$\begin{aligned} E_1 &= \frac{\pi\sqrt{2}u_0p_0}{8}\left(1+V_1^2\right) + \frac{3\left(\pi-2\right)\sqrt{2}u_0p_0^3C_{\rm nl}}{32} + \frac{\sqrt{2}\left(\pi+6\right)\lambda}{8p_0} \\ E_2 &= \frac{\left(6+\pi\right)\sqrt{2}\chi_2^2u_0^5}{16p_0\left(1-V_2^2\right)}\left(1+V_2^2\right) \\ E_3 &= \frac{\left(4+\pi\right)\sqrt{2}\chi_2u_0^5}{4p_0\left(V_2^2-1\right)}\left(1+V_2^2\right) \end{aligned} \tag{39}$$

and for the kinklike solitons and

$$\begin{aligned} E_1 &= \sqrt{2}u_0 p_0 \left(1+V_1^2\right)\left(\frac{\pi}{8}+\frac{1}{2}\right)+\frac{\sqrt{2}u_0 p_0^3 C_{\rm nl}}{16}\left(5+\frac{3\pi}{2}\right)+\frac{\sqrt{2}u_0\left(\pi+6\right)\lambda}{8p_0} \qquad (40)\\ E_2 &= \frac{\left(6+\pi\right)\sqrt{2}\chi_2^2 u_0^5}{16p_0\left(V_2^2-1\right)}\left(1+V_2^2\right)\\ E_3 &= \frac{\left(6+\pi\right)\sqrt{2}\chi_2 u_0^5}{8p_0\left(V_2^2-1\right)}\left(1+V_2^2\right) \end{aligned}$$

for the kink solitons with small hump near the center.

The width L of the kinklike soliton [shown in Fig.(10 a)] is estimated at 99% and is given by

$$L=\frac{\sqrt{2}u_0}{p_0}\left[\arcsin\left(\frac{\sqrt{2}u_1}{2u_0}\right)+ln\left(\frac{1}{2}\sqrt{4-2\left(\frac{u_1}{u_0}\right)^2}+\frac{\sqrt{2}u_1}{2u_0}\right)\right] \qquad (41)$$

where $u_1=\dfrac{99}{100}u_0$. Since Eq. (41) shows that the width of the kinks increases with the anharmonicity, thus this one will be able to only decrease with a strong coupling of the two sublattices [shown in Fig.(10 a)]. Let us estimate the width of the kink solution. Small displacements of the protons around the equilibrium position, involves a weak proton-proton interaction, order of the tenth of the force constant of the covalent bond of the OH. But, when the displacement of the proton is large, the interaction becomes strong, and the term $\frac{1}{4}mC_a\left(u_{n+1}-u_n\right)^4$ becomes the dominant contribution. Under these conditions we obtain $L\approx 3.7$ $\overset{\circ}{\rm A}$. Our numerical applications are carried out for ice at $T=263\ K$ (-10^oC). At this temperature, the lengths of the $O-H$ and $H\cdots O$ bonds are respectively 1.01 $\overset{\circ}{\rm A}$ and 1.75 $\overset{\circ}{\rm A}$. This gives for the lattice spacing a (e.g. the distance between two protons or two heavy-ions) the value $a=2.76$ $\overset{\circ}{\rm A}$ [57]. The distance u_0 along the chain from the top of the barrier to one minima in the double well potential is $u_0=0.39\overset{\circ}{\rm A}$ and the barrier $V_0=0.74\ eV$ [56]. The sound velocities C_0 for the proton sublattice and v_0 for the heavy-ion sublattice have the values $C_0=1.1\ 10^4\ m\cdot s^{-1}$ and $v_0=0.1C_0$. The masses of the particles are $m=1$ a.m.u (atomic mass unit) for the proton and $M=17$ a.m.u. for the heavy-ion. We have taken the particular value $\chi=30\ eV/\ \overset{\circ}{\rm A}^2$ for the coupling constant and $v=650\ ms^{-1}$ for the velocity. In Fig.(11), we have plotted the energy of kink solitons (see Eq.(39 against the coupling coefficient χ. In a general way, using the two-sublatice soliton-bearing model with anharmonic interaction, the energy and the width of the kink soliton, or other types of soliton patterns that we have obtained are much smaller than those of the previous models [31, 37, 54, 58, 59]. The kink solution obtained, involves about one and two protons only. Therefore, the present model seems to be more realistic and applicable to a system which consist of small number of hydrogen bonds.

3 Conclusions

In summary, we have presented a study of a nonlinear model for the motion of defects in quasi one-dimensional in hydrogen-bonded systems. The model extends previously two-sublattice

soliton-bearing one-dimensional models by the inclusion of anharmonicity in the study of lattice models. This is accomplished through the introduction of a quartic proton-proton interaction potential. The presence of nonlinear and linear dispersion terms, leads to soliton patterns of the model in the continuum limit, i.e., in the limit when only long-wavelength excitations are present. It was shown that in this limit, by applying two types of boundary condition, drop and condensate, and by considering the sign of the nonlinear proton-proton coupling, a rich analytic diversity of soliton patterns emerge, namely, peak, drop, bell, cusp, shock, kink, bubble and loop solitons. The total energy of all these coupled two-component soliton patterns has been calculated and decreases with the coupling of two sublattices when the interactions of the first one are of anharmonic forms. Another effect is related to a transition from closed to open phase trajectories of the system taking place beyond some threshold value of the lattice parameter, and/or the velocity of the soliton patterns. An exact analytical expression for the dependence of the breakdown threshold value on the nonlinear parameter, the velocity of soliton and on the parameter of coupling between the two sublattices, has been derived. These phenomena, for example, should contribute to the formation of cracks originating from dislocations observed [40] in semiconductor heterostructures. Impurities, as well as other defects, may locally influence the breakdown threshold and thus play a major role with respect to nonlinear excitations in such systems. The study of two-component soliton patterns in hydrogen-bonded chains taking into account lattice discreteness [54, 55, 27, 28] is now in progress.

Acknowledgments. This work was done within the framework of the Associateship Scheme of the Abdus Salam International Centre for Theoretical Physics, Trieste, Italy. A.S.T.N. would like to thank Professor Jan Govaerts for his materiel assistance and David Yemele for helpful discussions.

References

[1] V. Ya. Antonchenko, A. S. Davydov, A. V. Zolotaryuk, Phys. Status Solidi B **11**5, 631 (1983)

[2] M. Springborg, Phys. Rev. Lett. **59**, 2287 (1987)

[3] R. W. Jansen , R. Bertocini, D. A. Pinnick, A. I. Katz, R. C. Hanson, O. F. Sankey, M. O'Keeffe, Phys. Rev. B **35**, 9830 (1987)

[4] P. B. Hobbs, *Ice Physics*, (Clarendon, Oxford, 1974)

[5] J. F. Nagle, Morowitz, Proc. Natl. Acad. Sci. USA. **75**, 298 (1978)

[6] J. F. Nagle, Tristam-Nagle S, J. Membrane Biol. **74**, 1 (1983)

[7] N. Bjerrum , Science **115**, 385 (1952)

[8] J. F. Nagle, M. Mille, H. J. Morowitz, J. Chem. Phys. **72**, 3959 (1980)

[9] E. W. Knapp, K. Schulten, Z. Schulten, Chem. Phys. **46**, 215 (1980)

[10] D. DeVault, *Quantum-mechanical Tunneling in Biological Systems*, (Cambridge: Cambridge University Press, 1984)

[11] C. Branden and J. Tooze, *Introduction to Protein Structure*, (Garland: New York, 1991)

[12] I. A. Balabin, J. N. Onuchic, J. Phys. Chem. **100**, 11573 (1996).

[13] P. E. M. Siegbahn, M. R. A. Blomberg, R. H. Crabtree, Theor. Chem. Acc. **97**, 289 (1997)

[14] A. V. Zolotaryuk, K. H. Spatschek, E. W. Laedke, Phys. Lett. **101A**, 517 (1984)

[15] E. W. Laedke, K. H. Spatschek, M. Jr. Wilkens, A. V. Zolotaryuk, Phys. Rev. A **32**, 1161 (1985)

[16] St. Pnevmatikos Phys. Lett. **122A**, 249 (1987)

[17] S. Yomosa, J. Phys. Soc. Japan **52**, 1866 (1983)

[18] X. Duan, s. Scheiner, J. Mol. Struct. **270**, 173 (1992)

[19] X. Duan, S. Scheiner, Int. J. Quantum Chem., Quantum Biol. Symp. **19**, 109 (1992)

[20] X. Duan, S. Scheiner, R. Wang, Int. J. Quantum Chem., Quantum Biol. Symp. **20**, 77 (1993)

[21] E. S. Kryachko, Chem. Phys. **143**, 359 (1990)

[22] A. V. Zolotaryuk, St. Pnevmatikos, A. V. Savin, Physica D **51**, 407 (1991)

[23] A. V. Savin, A. V. Zolotaryuk, Phys. Rev. A **44**, 8167 (1991)

[24] R. Grauer, K. H. Spatschek, A. V. Zolotaryuk, Phys. Rev. E **47**, 236 (1993)

[25] O. Yanovitskii, G. Vlastou-Tsinganos, N. Flytzanis, Phys. Rev. B **48**, 12645 (1993)

[26] A.V. Zolotaryuk, M. Peyrard, K. H. Spatschek, Phys. Rev. E **62**, 5706 (2000)

[27] V. M. Karpan, Y. Zolotaryuk, P. L. Christiansen, A. V. Zolotaryuk, Phys. Rev. E **66**, 066603 (2002)

[28] V. M. Karpan, Y. Zolotaryuk, P. L. Christiansen, A. V. Zolotaryuk, Phys. Rev. E **70**, 056602 (2004)

[29] G. Kalosakas, a. V. Zolotaryuk, G. P. Tsironis, E. N. Economou, Phys. Rev. E **56**, 1088 (1997)

[30] St. Pnevmatikos, Phys. Rev. Lett. **60**, 1534 (1988)

[31] G. P. Tsironis, St. Pnevmatikos, Phys. Rev. B **39**, 7161 (1989)

[32] B. Dey, M. Daniel, J. Phys.: Condens. Matter **2**, 2331 (1990)

[33] E. S. Nylund, G. P. Tsironis, Phys. Rev. Lett. **66**, 1886 (1991)

[34] E. Simo, T. C. Kofane Physica Scripta **49**, 543 (1994)

[35] E. Simo, T. C. Kofane, Phys. Rev. E **54**, (1996)

[36] A. v. Zolotaryuk, K. H. Spatschek, A. V. Savin, Phys. Rev. B **54**, 266 (1996)

[37] Y. Kashimori, F. CHIEN, K. Nishimoto, Chem. Phys. **107**, 389 (1986)

[38] Y. Zolotaryuk, J. C. Eilbeck, J. Phys.: Condens. Matter **10**, 4553 (1998)

[39] N. K. Voulgarakis, G. P. Tsironis, Phys. Rev. B **63**, 014302 (2000)

[40] M. A. Ratner, B. G. Vekhter, Phys. Rev. B **51**, 3469 (1995)

[41] D. Hennig, Phys. Rev. E **61**, 4550 (2000)

[42] M. G. Velarde, W. Ebeling, A. P. Chetverikov, Int. J. Bifurcation and Chaos **15**, 245 (2005)

[43] M. G. Velarde, W. Ebeling, D. Hennig, C. Neissner, Int. J. Bifurcation and Chaos **16**, 1035 (2006)

[44] D. Hennig, C. Neisser, M. G. Velarde, W. Ebeling, Phys. Rev. B **73**, 024306 (2006)

[45] G. P. Agrawal, *Nonlinear fiber optics*, 2nd edn. (Academic: New York, 1995)

[46] P. Rosenau, J. M. Hyman, Phys. Rev. Lett. **70**, 564 (1993)

[47] P. Tchofo Dinda, T. C. Kofane, M. Remoissenet, Phys. Rev. E **60**, 7525 (1999)

[48] P. Tchofo Dinda, M. Remoissenet, Phys. Rev. E **60**, 6218 (1999)

[49] S. Dusuel S, P. Michaux, M. Remoissenet, Phys. Rev. E **57**, 2320 (1999)

[50] Kevrekidis, V. V. Konotop, A. R. Bishop, S. Takeno, J. Phys A:Math. Gen **35**, L641 (2002)

[51] A. S. Tchakoutio Nguetcho, J. R. Bogning, D. Yemele, T. C. Kofane, Chaos, Solitons and Fractals **21**, 165 (2004)

[52] M. A. Aguero, M. J. Paulin, Phys. Rev. E **63**, 046606 (2001)

[53] D. Hochstrasser, H. Buttner, H. Desfontaines, M. Peyrard, Phys. Rev. A **38**, 5332 (1988)

[54] R. Mefougue, P. Woafo, T. C. Kofane, Solid State Commun. **86**, 393 (1993)

[55] C. M. Ngabireng, P. Woafo, T. C. Kofane, Solid State Commun. **89**, 885 (1994)

[56] Xu Ji-Zhong, Solid State Commun **76**, 557 (1990)

[57] G. Pannetier, *Chimie Physique General. Atomique. Liaisons chimiques et structures molï¿½ulaires*, 3rd edn. (Masson, 1969)

[58] Y. Kashimori, T. Kikuchi, K. Nishimoto, J. Chem. Phys. **77(4)**, 1904 (198)

[59] P. Woafo, R. Takontchoup, A. S. Bokosah, J. Chem. Phys. Solids **56(9)**, 1277 (1995)

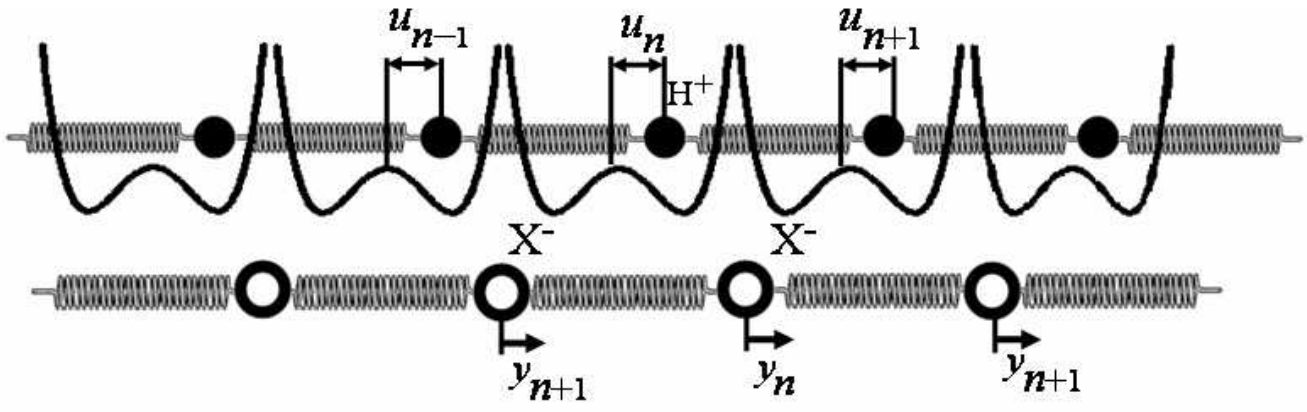

Figure 1: Schematic presentation of interactions in a chain of a $2C$ (C = Carbon) hydrogen bonded with double well potential curves.

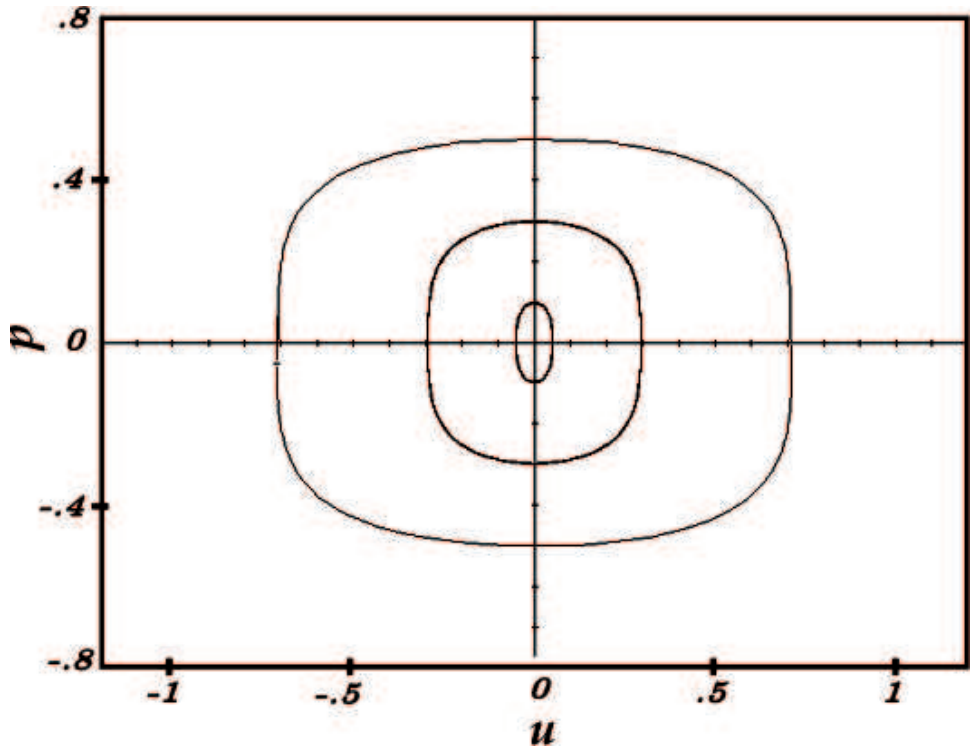

Figure 2: Phase trajectories $p(u)$ corresponding to the case $\eta > 1$ with $V_2 \in]0;1[$, or to the case $\eta < 1$ with $V_2 \in]V_{22};1[$, where $C_{\rm nl} > 0$ according to Eqs. (16), with $\eta = 3$, $u_0 = 1$, $V_2 = 0.5$, $V_1 = 0.5$, $\lambda = 1$ and $C_{\rm nl} = 25$.

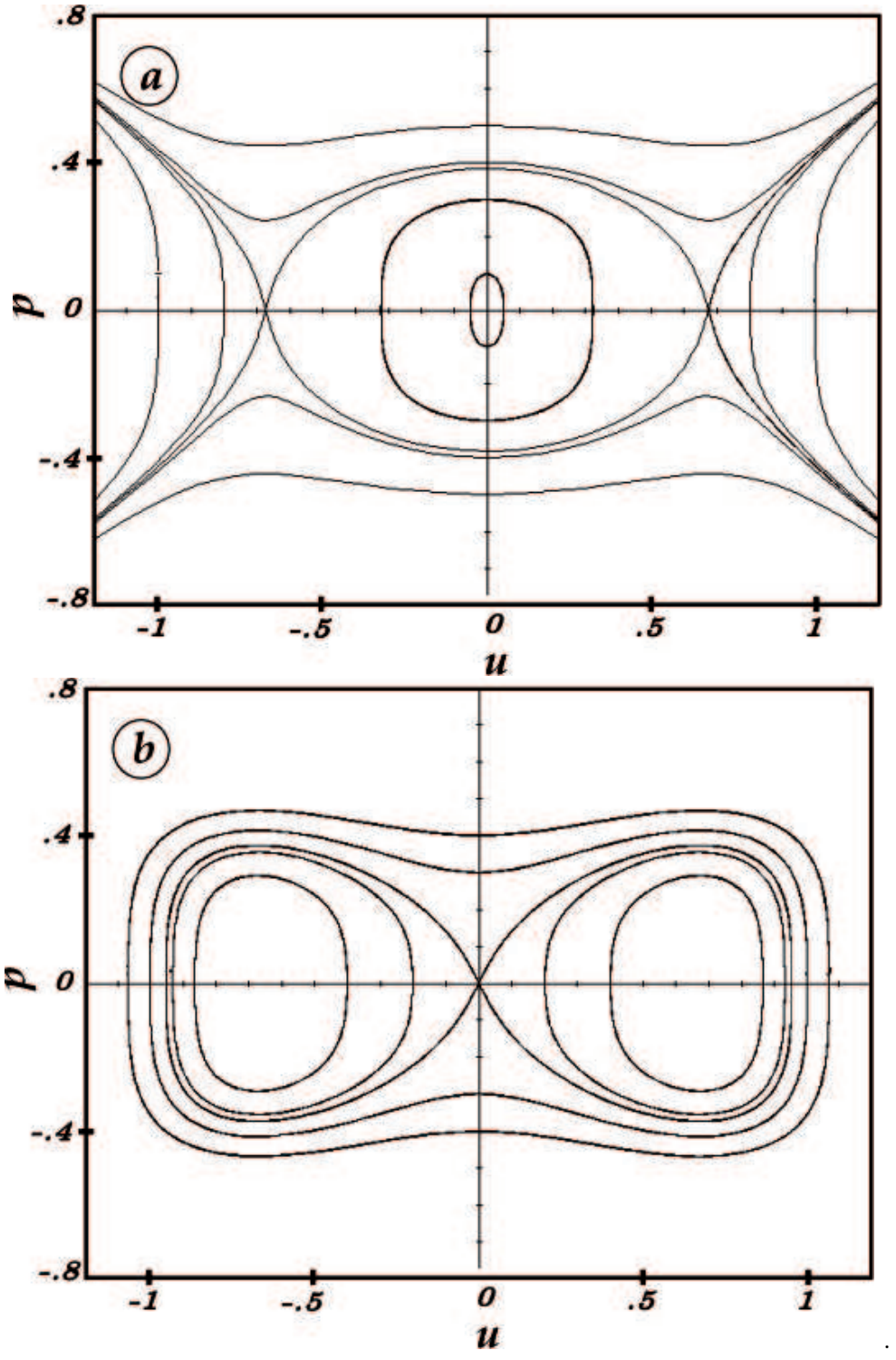

Figure 3: Phase trajectories $p(u)$ corresponding to the case: (a) $\eta > 1$ with $V_2 \in]1;\infty[$, or $\eta < 1$ with $V_2 \in]0;V_{22}[\cup]1;\infty[$ for positive values of $C_{\rm nl}$ and, (b) for negative values of $C_{\rm nl}$ according to Eqs. (16) for $\eta = 3$, $u_0 = 1$, $V_2 = 1.5$, $V_1 = 0.5$, $C_{\rm nl} = 25$ and $\lambda = 1$.

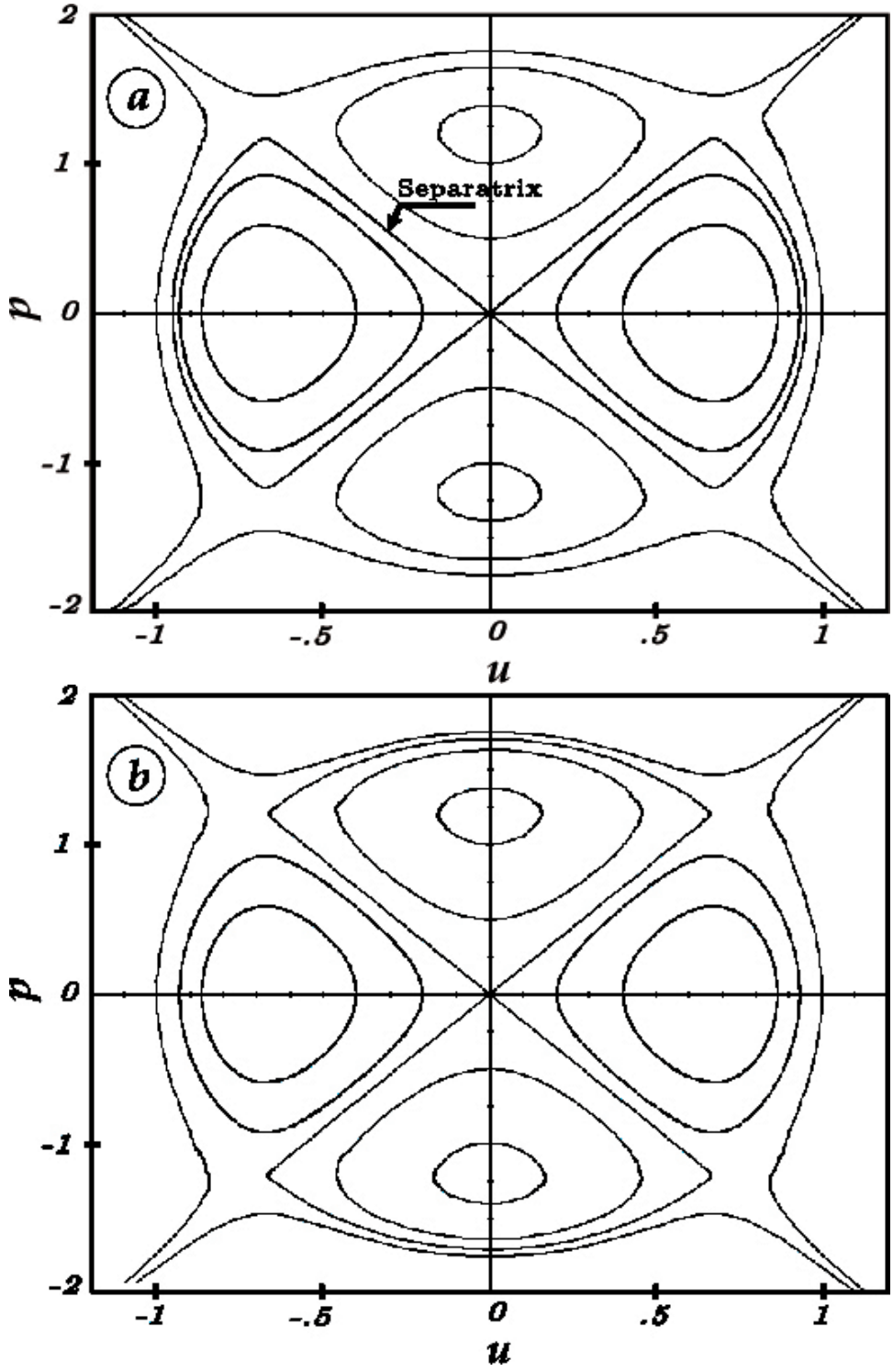

Figure 4: Change in phase trajectories $p\,(u)$ for two distinct values of the parameter that control the strength of the nonlinear coupling $C_{\rm nl}$, (a) $(C_{\rm nl} = 0.44) < C_{\rm nl_{cr1}}$, (b) $(C_{\rm nl} = 0.45) > C_{\rm nl_{cr1}}$, according to Eqs. (16) for $\eta = 3$, $u_0 = 1$, $V_2 = 1.5$, $V_1 = 1.5$, and $\lambda = 1$. That is $C_{\rm nl_{cr1}} \simeq 0.443$. In (a), we note the existence of separatrix and his rupture in (b) characterizing the disintegration of solitons.

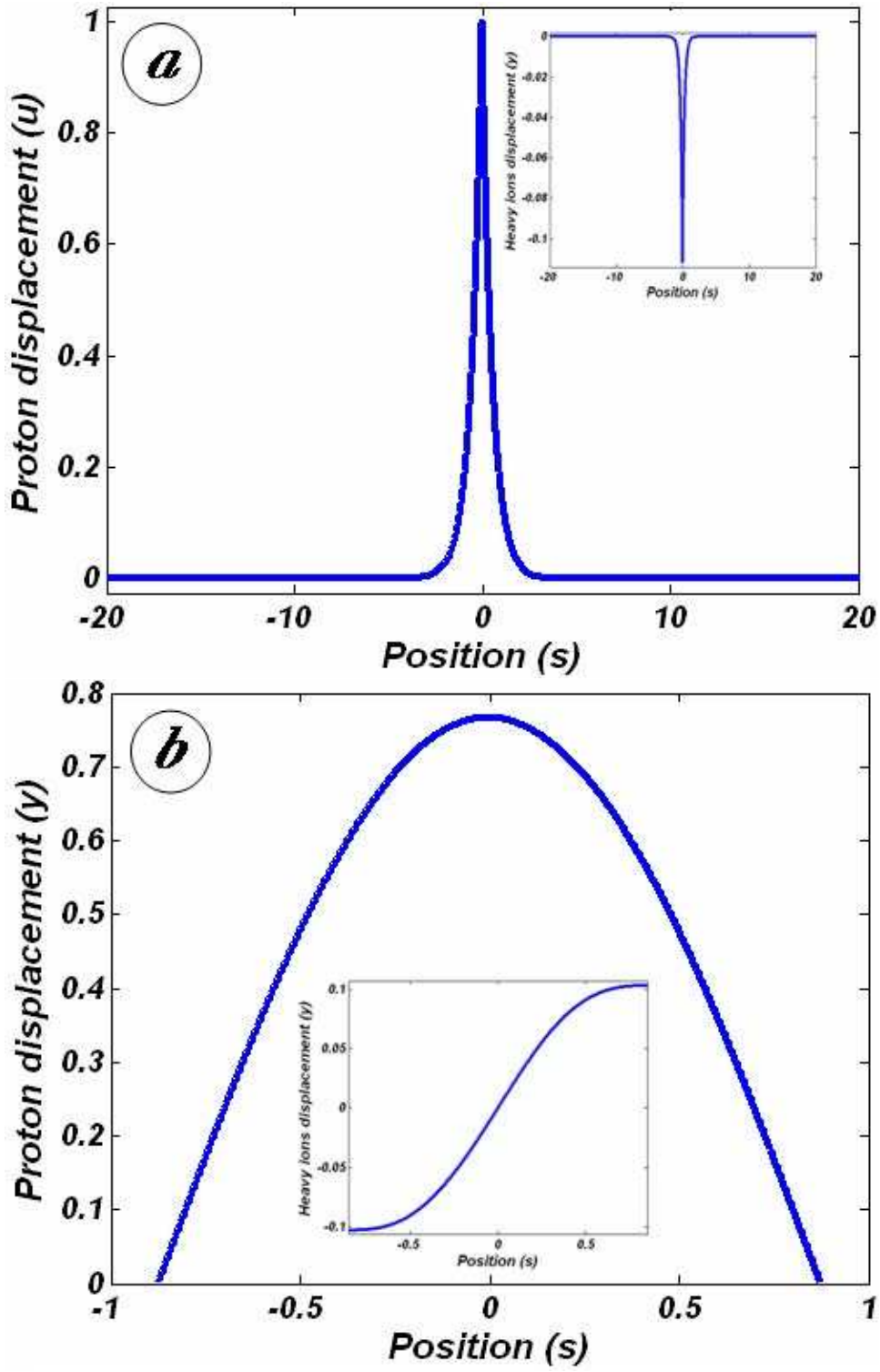

Figure 5: Representation of the field of two-component compact solutions u (for the proton) and y (for the hydroxyl) as a function of the position s, corresponding to the waveforms: (a) the peak solitons (peakons) and (b) the drop solitons, according to Eqs. (19) and Eqs. (21) respectively, with the condition Eqs. (18) for $\eta = 3$, $u_0 = 1$, $V_2 = 1.5$, $V_1 = 1.5$, $s_0 = 0$, $C_{nl} = 0.44$, $\chi 2 = 1$ and $\lambda = 1$.

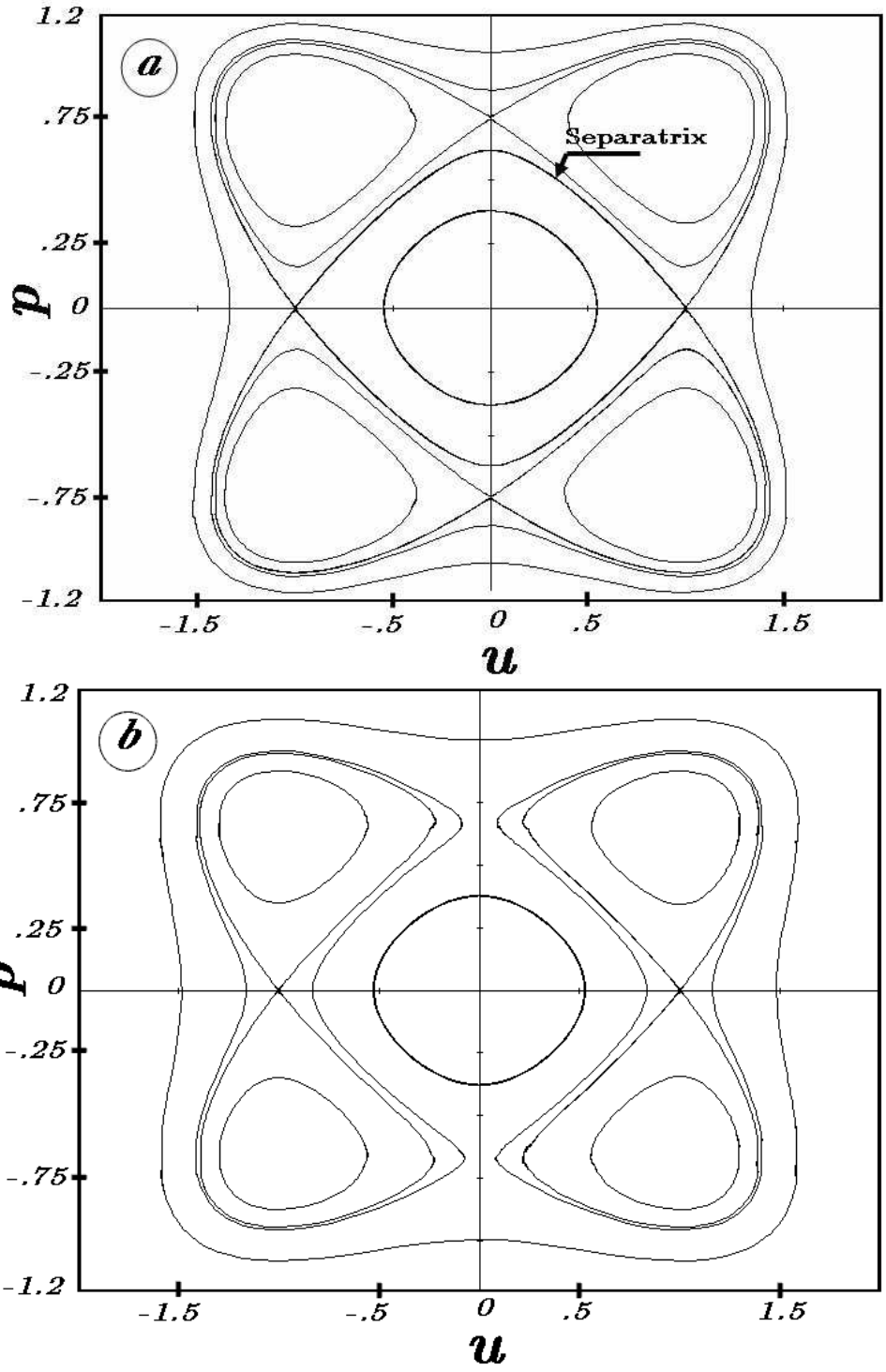

Figure 6: Change in phase trajectories $p\,(u)$ for two distinct values of the $C_{\rm nl}$, (a) $(C_{\rm nl}=14) < C_{\rm nl_{cr2}}$, (b) $(C_{\rm nl}=18) > C_{\rm nl_{cr2}}$, according to Eqs. (29) for $u_0=1$, $V_2=0.5$, $V_1=5$, $\eta=3$, and $\lambda=1$. That is $C_{\rm nl_{cr2}}=16$. In (a), we note the existence of separatrix and his rupture in (b) characterizing the disintegration of solitons.

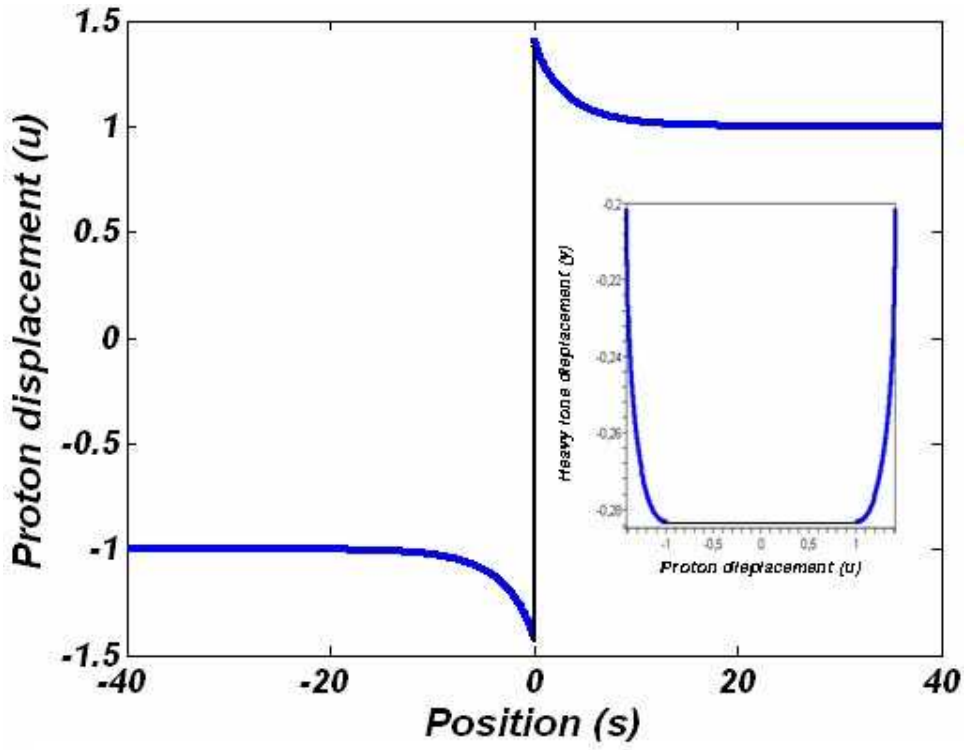

Figure 7: Representation of the field of soliton solutions u (for the proton) as a function of the position s, corresponding to the waveforms of the shock waves (because of the abrupt discontinuities that are observed when they are traveling). According to Eqs. (32) with the boundary condition Eqs. (33) for $s_0 = 0$, $m = 1$, $M = 16$, $v_0 = 2$, $C_0 = 1/5$, $\chi = 1.752$, $\lambda = 3/5$ and $u_0 = 1$.

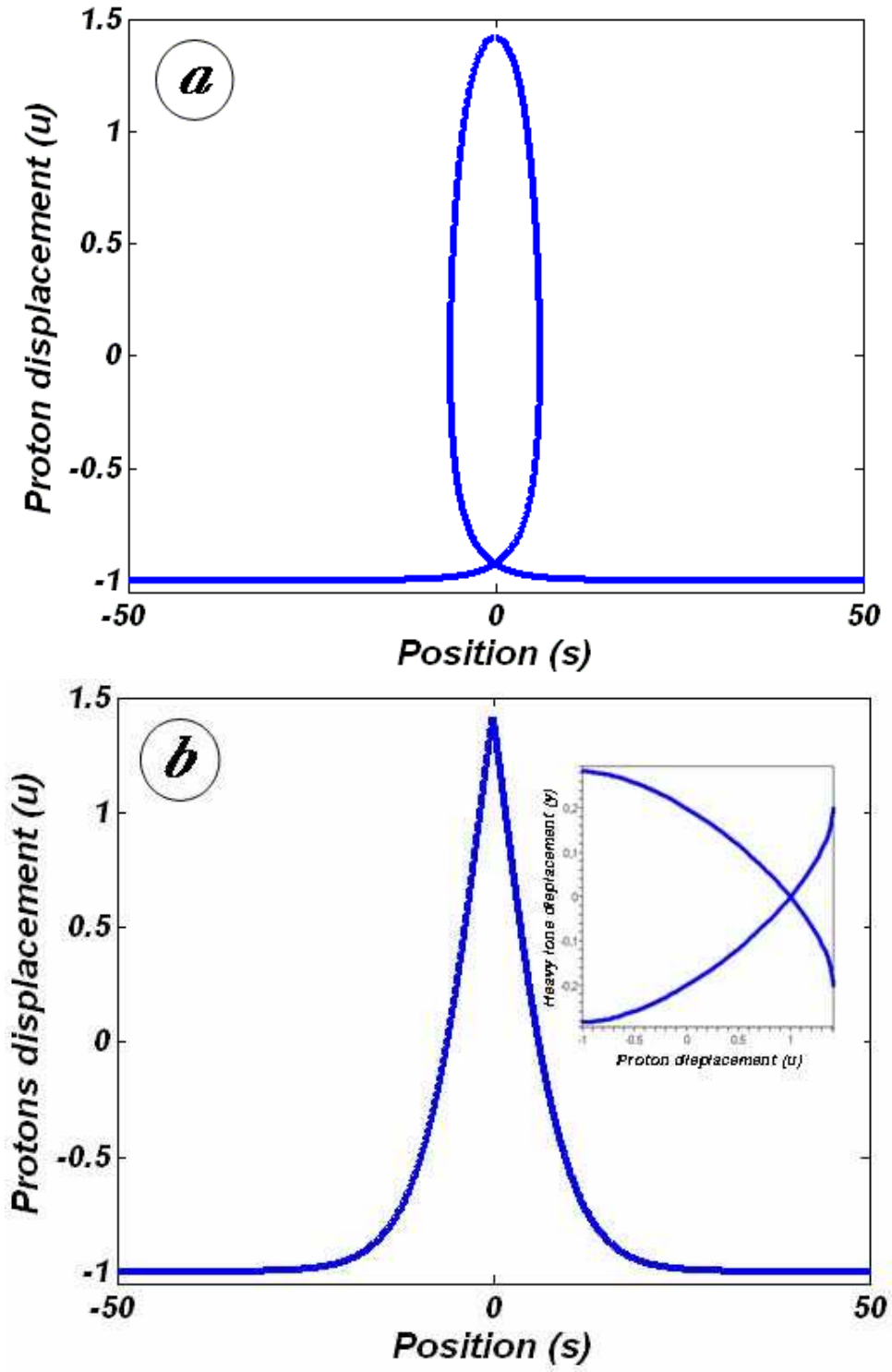

Figure 8: Representation of the field of soliton solutions u (for the proton) as a function of the position s, corresponding to the waveforms: (a) Loop soliton and (b), Typical peak soliton, according to Eqs. (32) with the boundary condition Eqs. (35) for $s_0 = 0$, $m = 1$, $M = 16$, $v_0 = 2$, $C_0 = 1/5$, $\chi = 1.752$, $\lambda = 3/5$ and $u_0 = 1$.

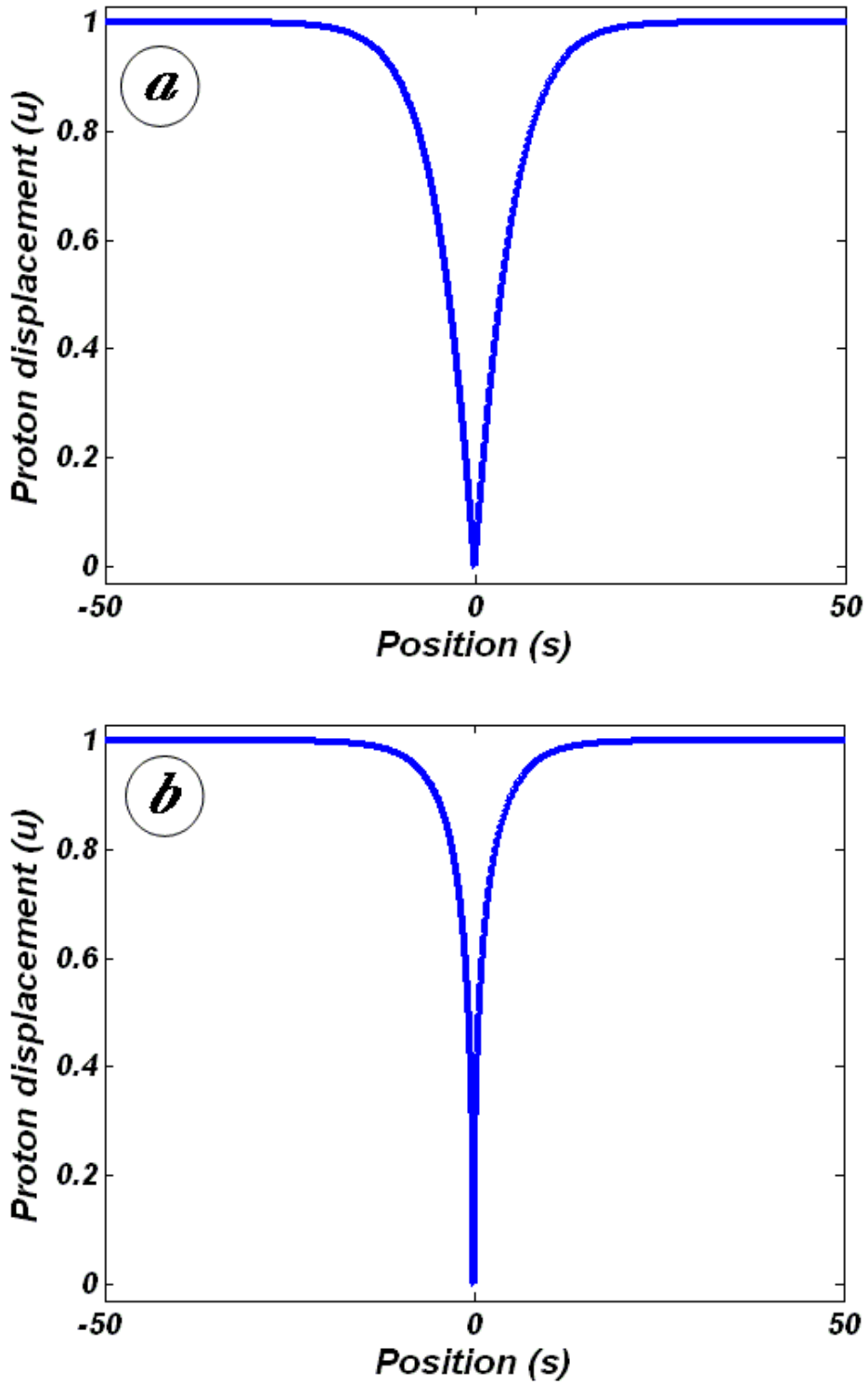

Figure 9: Representation of the field of bubble soliton solutions u (for the proton) as a function of the position s, corresponding to the waveforms, (a) Peak bubble (because of its rarefied form in the center) and (b) , Cusp solitons in the form of a straight bubble directed down that is an acute dip in the condensate according to Eqs. (32) with the boundary condition Eqs. (37) for $s_0 = 0$, $m = 1$, $M = 16$, $v_0 = 2$, $C_0 = 1/5$, $\chi = 1.752$, $\lambda = 3/5$ and $u_0 = 1$.

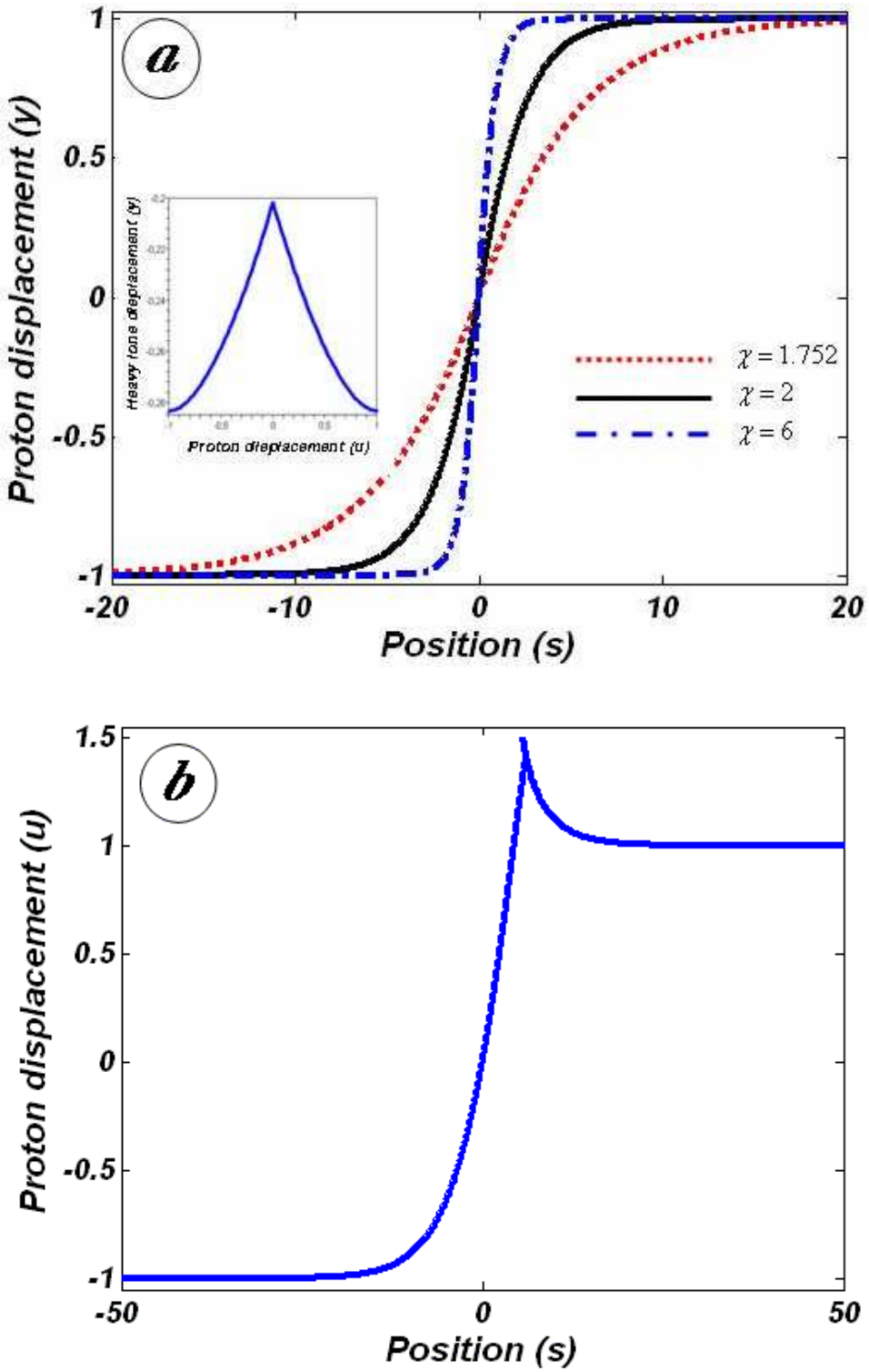

Figure 10: Representation of the field of soliton solutions u (for the proton) as a function of the position s, corresponding to the waveforms of the typical kinklike structure for different value of parameter of coupling of the two sublattices χ (a), and the kink soliton with small hump near its center (b), according to Eqs. (32) with the boundary condition Eqs. (33) for $s_0 = 0$, $m = 1$, $M = 16$, $v_0 = 2$, $C_0 = 1/5$, $\chi = 1.752$, $\lambda = 3/5$ and $u_0 = 1$.

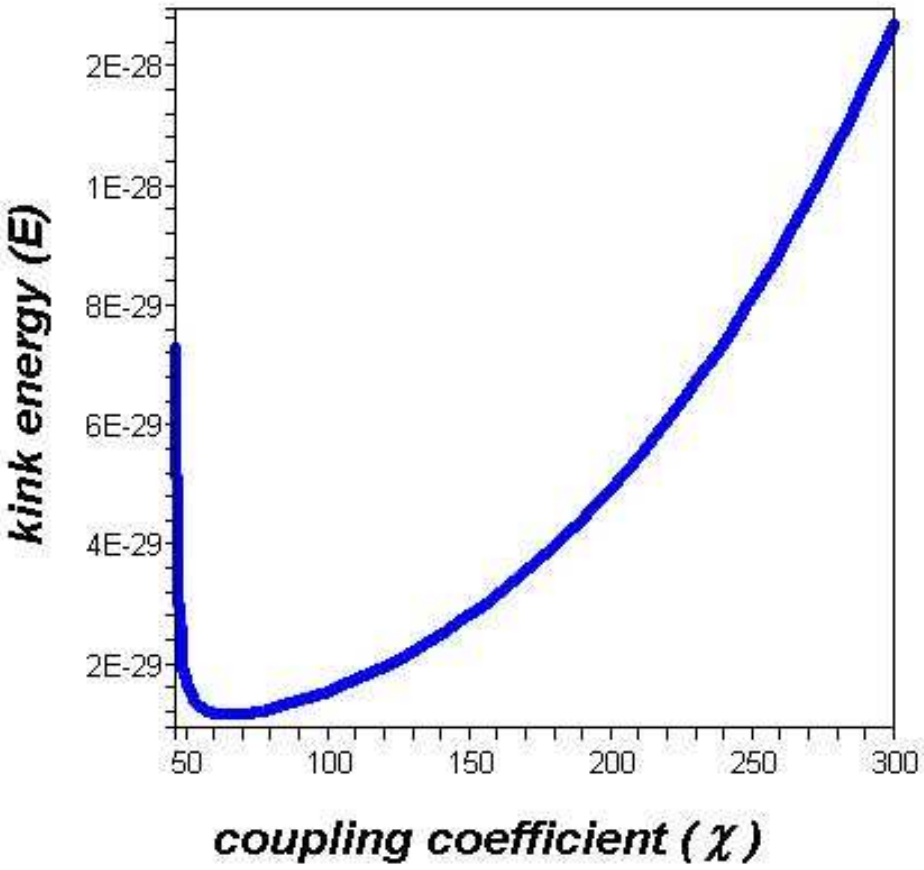

Figure 11: Variation of the kinks energy versus χ according to Eqs.(39) for $m = 1$ a.m.u, $M = 17m$, $C_0 = 1.1$ $10^4\ m \cdot s^{-1}$, $v_0 = 0.1C_0$, $V_0 = 0.74\ eV$, $u_0 = 0.39\mathring{\text{A}}$ and $v = 650\ ms^{-1}$.